CrossMark

MOLECULAR TOXICOLOGY

Activation of peroxisome proliferator-activated receptor α ameliorates perfluorododecanoic acid-induced production of reactive oxygen species in rat liver

Hui Liu[1] · Hongxia Zhang[1] · Ruina Cui[1] · Xuejiang Guo[2] · Dazhi Wang[3] · Jiayin Dai[1,3]

Abstract Perfluorododecanoic acid (PFDoA) is a ubiquitous environmental pollutant known to cause hepatocellular hypertrophy; however, the mechanisms of hepatotoxicity remain poorly understood. In this study, male rats were exposed to 0, 0.05, 0.2 and 0.5 mg/kg/day of PFDoA for 110 days. After two-dimensional differential gel electrophoresis and MALDI-TOF/TOF analysis, 73 differentially expressed proteins involved in lipid metabolism, inflammation, stress response and other functions were successfully identified. Among them, six significantly changed proteins (CTE1, MTE1, HADHA, ECH1, ALDH2 and CPS1) were found to be regulated by peroxisome proliferator-activated receptor alpha (PPARα). The anti-oxidant enzyme activity assays of superoxide dismutase and glutathione peroxidase and the content of thiobarbituric acid-reactive substances in the liver implied that PFDoA caused oxidative stress. The mRNA levels of PPARα in rat primary hepatocytes were knocked down by lentivirus-mediated RNAi. Furthermore, targeted protein levels of CTE1 and MTE1 were down-regulated, while those of HADHA, ALDH2 and CPS1 were up-regulated. After PFDoA exposure, however, the targeted protein levels of CTE1 and ALDH2 increased compared with those of the knockdown untreated group. The reactive oxygen species (ROS) content in rat hepatocytes assayed by flow cytometry significantly increased in the PPARα knockdown groups, consistent with the PPARα antagonist GW6471- and agonist WY14643-treated groups. These results strongly suggested that PPARα played an important role in suppressing ROS content in hepatocytes following PFDoA exposure.

Keywords Perfluorododecanoic acid (PFDoA) · Peroxisome proliferator-activated receptor alpha (PPARα) · Reactive oxygen species (ROS) · Lentivirus · RNAi

Hui Liu and Hongxia Zhang have contributed equally to this paper.

✉ Jiayin Dai
daijy@ioz.ac.cn

1 Key Laboratory of Animal Ecology and Conservation Biology, Institute of Zoology, Chinese Academy of Sciences, Beijing 100101, People's Republic of China

2 State Key Laboratory of Reproductive Medicine, Department of Histology and Embryology, Nanjing Medical University, Nanjing 210029, People's Republic of China

3 State Key Laboratory of Marine Environmental Science/ Environmental Science Research Center, Xiamen University, Xiamen 361005, People's Republic of China

Abbreviations

CTE1	Cytosolic acyl-CoA thioesterase 1, also known as Acot1 (acyl-CoA thioesterase 1)
MTE1	Mitochondrial acyl-CoA thioesterase 1, also known as Acot2 (acyl-CoA thioesterase 2)
HADHA	Hydroxyacyl-coenzyme A dehydrogenase/3-ketoacyl-coenzyme A thiolase/enoyl-coenzyme A hydratase (trifunctional protein), alpha subunit
ALDH2	Aldehyde dehydrogenase 2 family (mitochondrial)
ECH1	Enoyl CoA hydratase 1, peroxisomal
CPS1	Carbamoyl-phosphate synthetase 1
SOD	Superoxide dismutase
GPx	Glutathione peroxidase
TBARS	Thiobarbituric acid-reactive substances

Introduction

Perfluoroalkyl and polyfluoroalkyl substances (PFASs) are synthetic chemicals with high-energy carbon–fluorine bonds, which contribute to their high stability and low surface tension. Their unique properties have led to their broad application in various industrial and consumer products (Giesy and Kannan 2001). PFASs are highly persistent and difficult to biodegrade and therefore accumulate in the environment to levels that can be harmful to living systems (Dinglasan et al. 2004; Naile et al. 2010). Biomonitoring studies have revealed a global distribution of PFASs in environmental media, food, drinking water, wildlife and humans (Houde et al. 2011, 2006). Recent research noted that PFASs have become the highest exposed exogenous chemical in humans, exceeding that of more well-known environmental contaminants such as p,p'-dichlorodiphenyldichloroethylene and polychlorinated biphenyls (Thingholm et al. 2008). Perfluorooctanoic acid (PFOA, C8), perfluorooctansulfonate (PFOS, C8), perfluorononanoic acid (PFNA, C9) and perfluorododecanoic acid (PFDoA, C12) are the most commonly detected and studied PFASs of different carbon lengths (Calafat et al. 2007; Fujii et al. 2012; Senthilkumar et al. 2007).

The primary bioaccumulation and target organ of PFASs is the liver, where they can cause increased liver-to-body weight ratio and hepatocellular hypertrophy (Hundley et al. 2006; Seacat et al. 2003). Studies have shown that exposure to PFASs can also induce lower serum glucose levels, lower cholesterol levels and higher β-oxidation of fatty acids as well as induce adenoma in hepatocytes (Lau et al. 2007; Seacat et al. 2003; Shipley et al. 2004). However, the mode of action related to PFAS toxicity in rodents is not fully understood. Peroxisome proliferator-activated receptors (PPARs) are ligand-activated transcription factors, including three different PPAR subtypes (PPARα, PPAR β/δ and PPARγ) (Evans et al. 2004; Kersten et al. 2000). PPARα is highly expressed in the liver, and once activated can regulate the transcription of genes involved in a number of biological processes, including lipid metabolism, inflammation and cell growth. PPARγ is mainly expressed in the liver and white fat tissue (WAT) and is an activator of adipogenesis (Rosen et al. 1999). Recent studies showed that endogenous compounds, such as fatty acids and their eicosanoid derivatives, and synthetic agonists, such as PFASs, can be a kind of ligand to activate PPARs (DeWitt et al. 2009). Due to the structural resemblance of perfluorocarboxylic acids (PFCAs) to natural fatty acids, PFCAs can activate PPARα and are thought to be responsible for hepatomegaly, hepatic tumor induction and developmental toxicity in laboratory animals (Shipley et al. 2004; Takacs and Abbott 2007). However, PFCAs have also been found to induce hepatomegaly and neonatal toxicity in PPARα-null mice (Abbott et al. 2009; Takacs and Abbott 2007). These findings suggest that some toxic effect induced by PFCAs may be associated with a PPARα-independent mode of action; however, the detailed mechanisms still need to be investigated.

Many toxicological studies have analyzed the liver toxicity of eight-carbon PFCAs (e.g., PFOA). In most wildlife tissues, however, long-chain PFCAs dominate the overall PFCA profile (Martin et al. 2004) due to their greater bioaccumulation factors (Lin et al. 2014; Martin et al. 2003). Despite this, limited studies have been conducted on longer-chain PFCAs. Several studies showed that PFDoA was a greater accumulator than PFOA in water, sediment and liver samples of selected species (Lam et al. 2014). In earthworms from industrially impacted soil, for example, the highest PFDoA concentrations reached 737 ng/g ww (Rich et al. 2015). In addition, longer carbon chain PFCAs was found to be more toxic than shorter carbon chain compounds (Kudo et al. 2001, 2006; Ohmori et al. 2003). Increased cell toxicity with increasing PFAS carbon chain length was also confirmed in different cells (Gorrochategui et al. 2014; Kleszczynski et al. 2007; Liu et al. 2008). However, few studies have focused on the toxic mechanism of long-chain PFCAs.

Proteomic technologies have been successfully used in the toxicology field and provide insight into the mechanisms of toxic compounds (Wetmore and Merrick 2004). Two-dimensional differential gel electrophoresis (2-D DIGE) efficiently and accurately separates proteins in complex mixtures and quantifies differential expression in treated and control samples (Alban et al. 2003). This technology is useful as a broad-based screening tool to analyze environmental stress responses in organisms.

To better understand the underlying hepatotoxicity mechanism of PFDoA, we performed 2-D DIGE followed by mass spectrometric analyses of rat liver both with and without chronic PFDoA exposure. Furthermore, based on proteomics discovery, we used lentivirus-mediated RNAi to knockdown PPARα expression in rat primary hepatocytes in vitro to elucidate its role in the mechanism of hepatotoxicity caused by PFDoA exposure.

Methods

Chemicals and standards

PFDoA (CAS No. 307-55-1, 95 % purity) was purchased from Sigma-Aldrich (St. Louis, MO, USA). $^{13}C2$-PFDoA (≥95 % purity) was purchased from Wellington Laboratories (Ontario, Canada). Tetra-n-butylammonium hydrogen sulfate (TBA), methyl-tert-butyl ether (MTBE), sodium carbonate, methanol, ammonium acetate (97 %),

ammonium solution (25 %) and acetic acid (99.9 %) were obtained from Wako Pure Chemical Industries (Osaka, Japan).

Animal treatments

Forty male Sprague–Dawley rats (200 ± 10 g) were obtained from the Vital River Laboratories (Beijing, China). The animals were maintained in a SPF grade facility on a 12-h light/12-h dark cycle and were allowed ad libitum access to a standard diet and pure water. The ambient temperature in the animal room was 23 ± 1 °C, and the relative humidity was 60 ± 5 %. After 1 week of adaptation, the rats were randomly separated into four groups of ten animals each. PFDoA was dissolved in 0.2 % Tween-20. The treatment rats were given doses of 0.05, 0.2 and 0.5 mg PFDoA/kg body weight/day by oral gavage for 110 days. The control animals were also treated with vehicle (0.2 % Tween-20), accordingly. At the end of the experiment, six rats from each group were weighed and killed by decapitation; the other four rats from each group were used for another study. The liver was rapidly sampled, weighed, rinsed with PBS and divided into small aliquots, flash frozen in liquid nitrogen and stored at −80 °C until further analysis. All procedures were performed in accordance with the Ethics Committee of the Institute of Zoology, Chinese Academy of Sciences.

PFDoA extraction and concentration quantification in liver

Extraction of PFDoA from liver samples was carried out using an ion pairing method described elsewhere (Hansen et al. 2001), and the final ion pairing extract was then subjected to a further cleanup process using a SPE-Oasis®-WAX method (Taniyasu et al. 2005). The PFDoA concentration in liver was analyzed using high-performance liquid chromatography with tandem mass spectrometry (HPLC–MS/MS). Detailed information is given in the Supporting Information (SI).

Protein preparation and CyDye labeling

Total protein was extracted from the liver using sample lysis buffer [7 M urea, 2 M Thiourea, 30 mM Tris, 4 % (w/v) CHAPS, 1 mM PMSF and 1 % protease inhibitor cocktail (Sigma-Aldrich, St. Louis, MO, USA)]. Cellular debris was removed by centrifugation at 4 °C for 20 min at 12,000g. Protein concentration was determined using the 2-D Quant protein assay kit (GE Healthcare, Uppsala, Sweden).

Three groups (0, 0.2 and 0.5 mg/kg/day PFDoA) were chosen for DIGE analysis based on previously observed

changes in gene expression in the liver and clinical chemistry parameters (Ding et al. 2009). Equal amounts of protein sample from two randomly selected rats in the same treatment group were pooled and further purified using the 2-D Clean-Up kit (GE Healthcare) for subsequent DIGE analysis. Each group yielded three pooled protein samples, and the pH values of the desalted samples were adjusted to 8.5 with 100 mM sodium hydroxide before labeling. The internal standard (IS) was comprised of a pool of an equal amount of all experimental samples. A total of 50 μg of protein from the controls and all treated groups was labeled with 400 pmol of either Cy3, Cy5 or Cy2 (Cy2 was used to label the IS) according to the manufacturer's recommended protocols (GE Healthcare). The labeled mixtures were combined according to Table S1 (in the SI) and were then adjusted to 450 μl with rehydration buffer (7 M urea, 2 M thiourea, 2 % CHAPS, 0.5 % IPG buffer 4–7 and a trace of bromophenol blue) prior to isoelectric focusing (IEF) and subsequent SDS-PAGE.

2-D DIGE and MALDI-TOF/TOF analysis

The labeled mixtures were loaded onto Immobiline dry strips (24 cm, linear pH gradient from 4 to 7, GE Healthcare). The IPG strips were rehydrated overnight at 40 V for 5 h followed by 100 V for 6 h, and IEF was then conducted for a total of 78 kVh on a Multiphor II system (GE Healthcare). After completion of the IEF program, the strips were equilibrated and then applied to 12.5 % polyacrylamide gels using Ettan™ Dalt six equipment (GE Healthcare). All electrophoresis procedures were performed in the dark and run in duplicate. Gels were scanned using a Typhoon™ Trio Series Variable Mode Imager (GE Healthcare) at 100 μm resolution, followed by silver staining. The resulting gel images were analyzed using DeCyder software 6.5 (GE Healthcare). BVA revealed differences between PFDoA-treated groups and the control group across all gels. Student's t test was used to statistically analyze the data, with $p < 0.05$ considered statistically significant.

Protein spots with significantly altered expression levels between the control and treated groups were manually excised from silver-stained gels for digestion and identification by an ABI 4700 MALDI-TOF/TOF Proteomics Analyzer (Applied Biosystems, Framingham, MA, USA) according to our previous studies (Zhang et al. 2011, 2012). Detail methods and parameters were given in the SI.

Bioinformatics analysis

Gene functional categorization and pathway analysis were performed with DAVID Bioinformatics Resources 2008 (http://david.abcc.ncifcrf.gov/), which provides a gene module level annotation of proteins rather than the specific

function of every protein. The annotated proteins are clustered according to the biological process branch of the GO annotation using. An analysis of diseases associated with proteins differentially expressed in the liver compared with the control rat liver was performed using Pathway-Studio™ (v5.0) software (Ariadne Genomics, Inc., Rockville, MD, USA). This text-mining software uses a database assembled from scientific abstracts and a manually curated dictionary of synonyms to recognize biological terms (Nikitin et al. 2003).

Anti-oxidant enzyme activity assay

One gram of liver tissue was homogenized in 0.9 ml of cold physiological saline solution. After centrifugation (2000g, 20 min at 4 °C), the supernatant was collected for further analysis. The activities of superoxide dismutase (SOD), glutathione peroxidase (GPx) and catalase (CAT) were measured using relevant kits (Nanjing Jiancheng Bioengineering Institute, China) according to the manufacturer's instructions. Lipid peroxidation content in terms of thiobarbituric acid-reactive substances (TBARS) formation was measured using a TBARS kit (Cayman Chemical Company, USA) according to the manufacturer's instructions.

Isolation and culture of rat primary hepatocytes

Rats were anesthetized by intraperitoneal injection of sodium pentobarbital (45 mg/kg). Primary hepatocytes were isolated by the two-step in situ collagenase perfusion technique, as described previously (Seglen 1976; Shen et al. 2012). The viability of hepatocytes was more than 95 % as assessed by trypan blue dye. Afterward, rat primary hepatocytes were plated onto six-well plates at a density of 1×10^6 cells/well and cultured in Williams E medium containing 10 % fetal bovine serum and primary hepatocyte maintenance supplements (1 kit per 500 ml medium, Gibco, Life Technology, USA) at 37 °C in a humidified atmosphere of 95 % air and 5 % CO_2.

3-(4,5-Dimethylthiazol-2-yl)-2,5-diphenyltetrazolium bromide (MTT) assay

The effect of PFDoA on the viability of hepatocytes was evaluated by MTT proliferation assay. Exponentially growing cells were seeded into a 96-well plate at a density of 1.0×10^4 cells/well in triplicate. After incubation for 24 h, cells were treated with increasing concentrations of PFDoA (1–100 µM in ethanol) for 20 h. Then, 20 µl of 5 mg/ml MTT was added to each well, followed by incubation for an additional 4 h. The formazan grains formed by viable cells were solubilized with dimethylsulfoxide (DMSO), and the color intensity was measured at 490 nm using a Gen5 Microplate reader (BioTek® Instruments, Inc., USA).

Lentiviral RNAi plasmid construction

To knockdown PPARα gene expressions, four miRNA RNAi sequences targeting PPARα (Table S2 in the SI) were cloned into pcDNA™6.2-GW/EmGFPmiR vector using a BLOCK-iT™ Pol II miR RNAi Expression Vector Kit with EmGFP (Invitrogen Life Technology, USA) and co-transfected into HEK293 cells with the corresponding overexpression plasmid. The best RNAi vectors were subcloned into pLenti6.3/V5-DEST vectors (Invitrogen Life Technology) by the GateWay recombination method. The constructed lentiviral RNAi plasmids were transfected into *Escherichia coli* Stbl3 cells (Invitrogen Life Technology), and the plasmids were extracted by a PureLink® HiPure Plasmid Filter Maxiprep Kit (Invitrogen Life Technology).

Preparation of lentivirus

Recombinant lentiviruses were prepared by co-transfecting 293FT cells with lentivirus expression plasmid with the ViraPower™ lentiviral expression system (Invitrogen Life Technology) using Lipofectamine 2000. Infectious lentiviruses were harvested at 48 and 72 h post-transfection and then filtered through 0.22 µm PVDF filters. The viruses were concentrated by ultracentrifugation. Viral titer was estimated by infecting 8×10^3 293FT cells with tenfold serial dilutions of virus stock with 4 µg/ml polybrene in a 96-well plate. The percentage of green fluorescent protein (GFP) positive cells was determined by counting cells at 20× magnification and used to calculate the number of transducing units per milliliter of viral supernatant (TU/ml). GFP expression in infected cells was observed using an inverted fluorescence microscope (Nikon Eclipse Ti-S, Japan), and images were captured using Nis-elements F package software (Nikon, Japan). The virus titers were at the range of 10^8 TU/ml.

Hepatocyte transduction and PFDoA exposure

Rat primary hepatocytes were plated at a density of 1×10^6 cells/well in six-well plates at 37 °C in a humidified atmosphere of 95 % air and 5 % CO_2. After overnight incubation, hepatocytes were incubated with lentivirus at a multiplicity of infection (MOI) of 30 without polybrene. For pseudo-transduction control (mock infections), hepatocytes were incubated with lentivirus with a scramble sequence at an MOI of 30. After 12-h incubation, media containing lentivirus were removed and replaced by new Williams E media containing 10 % fetal bovine serum and primary hepatocyte maintenance supplements. At 96 h post-transduction, transduction efficiency was examined under an inverted fluorescence microscope (Nikon Eclipse Ti-S, Japan). If transduction succeeded, PFDoA was added to the culture media at 75 µM, and control

and vehicle (ethanol) control were included, accordingly. Hepatocytes were rinsed with DPBS after 24 h of PFDoA exposure and harvested for subsequent real-time PCR and western blot assays. Total mRNA was extracted using Trizol (Ambion Life Technology, NY, USA) according to the manufacturer's instructions. Real-time PCRs were performed to investigate the knockdown efficiency of peroxisome proliferator-activated receptor alpha (PPARα).

Western blot analysis

Total proteins were extracted with RIPA (Thermo Scientific, USA) containing 1 mM PMSF (Sigma-Aldrich, USA) and 1 % phosphatase inhibitor (F. Hoffmann-La Roche Ltd, Switzerland). The protein concentration was determined using a BCA kit (Pierce, Thermo Scientific, USA). Approximately 40 μg of total protein was loaded on 10 % sodium dodecyl sulfate (SDS)-polyacrylamide gels and then transferred to polyvinylidene fluoride (PVDF) membranes (Amersham Biosciences, Piscataway, NJ, USA). The blotted membranes were blocked for 1 h in TBS containing 0.1 % Tween-20 (TBST) and 5 % BSA (Amresco, USA) and then incubated with primary antibodies dissolved by TBST overnight at 4 °C. The primary antibodies included rabbit monoclonal antibodies to rat cytosolic or mitochondrial acyl-CoA thioesterase 1 (CTE1/MTE1, from Dr. Yamada, Tokyo University of Pharmacy and Life Sciences, Japan); rabbit monoclonal antibodies to rat PPARα; hydroxyl acyl-coenzyme A dehydrogenase/3-ketoacyl-coenzyme A thiolase/enoyl-coenzyme A hydratase (trifunctional protein), alpha subunit (HADHA); enoyl CoA hydratase 1, peroxisomal (ECH1) and carbamoyl-phosphate synthetase 1 (CPS1) (Abcam, UK); mouse monoclonal antibodies to rat aldehyde dehydrogenase 2 family (ALDH2), human isovaleryl coenzyme A dehydrogenase (IVD, Proteintech Group, Chicago, IL, USA), rat malate dehydrogenase 1 (MDH1, AVIVA, Beijing, China), rat dihydrolipoamide S-acetyltransferase (DLAT, AVIVA, Beijing, China), rat glyceraldehyde-3-phosphate dehydrogenase (GAPDH, CST, USA) and rat hypoxanthine–guanine phosphoribosyltransferase (Hprt, Santa Cruz, USA). After washing with TBST, the membranes were then incubated with horseradish peroxidase-conjugated anti-rabbit IgG as the secondary antibody for 1 h at room temperature. The immunoreactive bands were detected with an ECL reagent (Tiangen, China) on an Image Quant LAS 4000 instrument (GE Healthcare, USA).

Reactive oxygen species (ROS) measured by flow cytometry

Rat hepatocytes were pre-treated with either PPARα antagonist (GW6471, 10 μM) or PPARα agonist (WY14643,

100 μM) for 24 h, respectively, then exposed to 0 or 75 μM PFDoA. The ROS content was assayed by ROS-sensitive dye H$_2$DCFDA (Molecular Probes, Life Technologies, USA). For the PPARα knockdown experiment, rat hepatocytes were infected by lentiviruses (Lenti-miPPARα and Lenti-NC) and exposed to 0 or 75 μM PFDoA. The ROS content was assayed by ROS-sensitive dye dihydroethidium (DHE) (Sigma-Aldrich, St. Louis, MO, USA). ROS content was measured by flow cytometry (BD FACSCalibur, Becton-Dickinson, San Jose, CA, USA). Totally, 10,000 cells were counted for each sample, and only double positive cells (GFP transduced by lentivirus and red color stained by DHE probe) were selected for ROS measurement.

Statistical analysis

For quantitative real-time PCR data and western blot analyses, statistical significance was determined using one-way analysis of variance (ANOVA) followed by Duncan's multiple range test (SPSS for Windows 17.0 Software, Inc., Chicago, IL, USA). Data are presented as means with standard errors (mean ± SE). A p value of <0.05 was considered statistically significant.

Results

PFDoA concentration in liver

After PFDoA exposure, PFDoA bioaccumulation in the rat liver increased in an obvious dose-related manner. The liver PFDoA concentration in the 0.5 mg/kg PFDoA/day group was 151.7 μg/g wet, a 583.3-fold increase compared with that of the control and a 4.79-fold increase compared with that of the 0.05 mg/kg PFDoA/day group (Fig. S1 in the SI).

2-D DIGE analysis for liver proteins

We used 2-D DIGE to explore the effect of PFDoA on the global pattern of protein expression in the rat liver. A representative example of the 2-D DIGE gel images with three channels is shown in Fig. S2 in the SI, demonstrating effective separation of proteins. Through spot detection with the DIA module of the DeCyder software, the number of spots on each 2-D DIGE gel was above 1600. Among these proteins, 143 and 275 spots were significantly altered (as determined by BVA module analysis) in the 0.2 and 0.5 mg/kg/day PFDoA groups, respectively, compared with the control rats ($p < 0.05$). A total of 80 proteins were significantly altered in both treatments. In total, 159 and 179 proteins were up- and down-regulated, respectively, compared with those in the control (Fig. S3 in the SI). After MALDI-TOF/

TOF analysis and a MASCOT database search, 73 proteins, including 53 up-regulated and 21 down-regulated proteins, were identified (Fig. S3 in the SI), Interestingly, 70 of these proteins changed significantly in their expression levels in the 0.5 mg/kg/day PFDoA group, with three identified proteins significantly changed in 0.2 mg/kg/day PFDoA group only ($p < 0.05$, Table S3 in the SI). In addition, some spots were identified as the same protein by TOF/TOF; for example, spots 410, 417 and 429 were all identified as Hsp60, which was verified by western blot analysis (Fig. S3, in the SI). This overlap might be due to differences in post-translational modifications, which can change the isoelectric point (PI) of a protein.

To further study the action mechanism of PFDoA on the rat liver, we classified the 73 identified proteins by GO analysis according their biological processes or functions (Table S3, in the SI). Most proteins were involved in lipid metabolism, amino acid metabolism, tricarboxylic acid (TCA) cycle and pyruvate metabolism, gluconeogenesis and glycolysis, stress response, cytoskeleton-related proteins and other functions.

In addition, we analyzed the disease network regulated by the PFDoA altered proteins using Pathway Studio software. Results showed that 18 altered proteins were related to hepatoma, adenocarcinoma, liver cancer or adenoma (Fig. S4, in the SI), and 21 altered proteins were related to inflammation (Fig. 1a). For example, adenosine kinase (ADK) peroxiredoxin 2 (Prdx2) and Prdx4, two proteins of the anti-oxidative function Prdx family, were recently found to have functions in inflammation, cancer and innate immunity (Ishii et al. 2012; Yamada et al. 2012).

The interaction relationship results showed that six proteins (MTE1, HADHA, CET1, ALDH2, ECH1 and CPS1) were regulated by PPARα and seven proteins (GPD1,

Fig. 1 Analysis of regulatory network of all differentially expressed proteins identified in the rat liver. Pathway analysis was performed using Pathway Studio (v 7.0) software. **a** Network of proteins related to inflammation. **b** Analysis of regulatory network of PPARα and PPARγ downstream proteins, which were differentially expressed in the rat liver
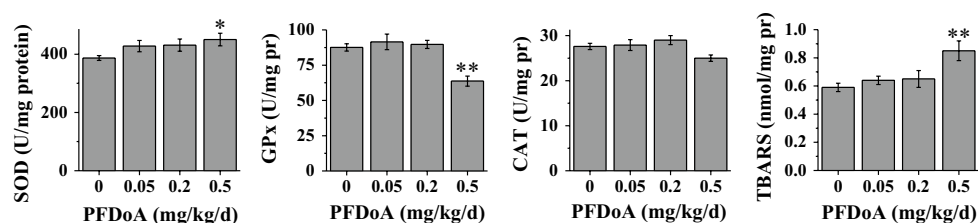
Fig. 2 Anti-oxidative enzyme active assay in rat livers chronically exposed to PFDoA. Chronic PFDoA exposure induced changes in the activity of anti-oxidant enzymes in the liver. Activity levels of major anti-oxidant enzymes, such as SOD, were significantly increased in the 0.5 mg/kg/day PFDoA group; GPx significantly decreased and content of thiobarbituric acid-reactive substances (TBARS), which correlated with lipid peroxidation, significantly increased in the 0.5 mg/kg/day PFDoA group

DDAH1, ALDH9A1, IL6, HPX, KRT8 and PHB) were regulated by PPARγ either directly or indirectly (Fig. 1b). Serum albumin was regulated by both PPARα and PPARγ.

Most proteins involved in stress response were heat-shock proteins (HSPs), including heat-shock 70kD protein 5 (HSPA5), heat-shock protein 1 (HSPD1), heat-shock protein 8 (HSPA8) and 75kD glucose-regulated protein (HSPA9A), the protein expression levels of which were all induced by PFDoA, as well as tumor necrosis factor type 1 receptor-associated protein (TRAP) was also induced by PFDoA. The expression levels of peroxiredoxin 2 (PRX2), peroxiredoxin 4 (PRX4) and thioredoxin domain containing 7 (PDIA6), which play critical roles in the elimination of ROS, were down-regulated in the PFDoA groups.

To verify the authenticity of the 2-D DIGE proteomic results, we analyzed several selected proteins involved in lipid metabolism, oxidation stress and other biological processes by western blot analysis. IVD was involved in amino acid metabolism, and DLAT and MDH1 were important enzymes in the TCA cycle and glucose metabolism. The protein levels of the above proteins increased or decreased in similar patterns to those observed in the DIGE results ($p < 0.05$, Fig. S5A, B in the SI), indicating that the 2-D DIGE results were reliable.

Activities of anti-oxidative enzymes and activation of PPARα in rat liver after chronic PFDoA exposure

Since the proteomic results implied that PFDoA exposure might cause inflammation and oxidative stress in the liver, we further assayed the activities of anti-oxidative enzymes in the liver. The activity of SOD was increased significantly in the 0.5 mg/kg/day group ($p < 0.05$), while the activity of GPx was decreased significantly ($p < 0.01$) and the content of TBARS was significantly increased ($p < 0.01$) (Fig. 2). These results implied that chronic PFDoA exposure caused oxidative stress in the rat liver.
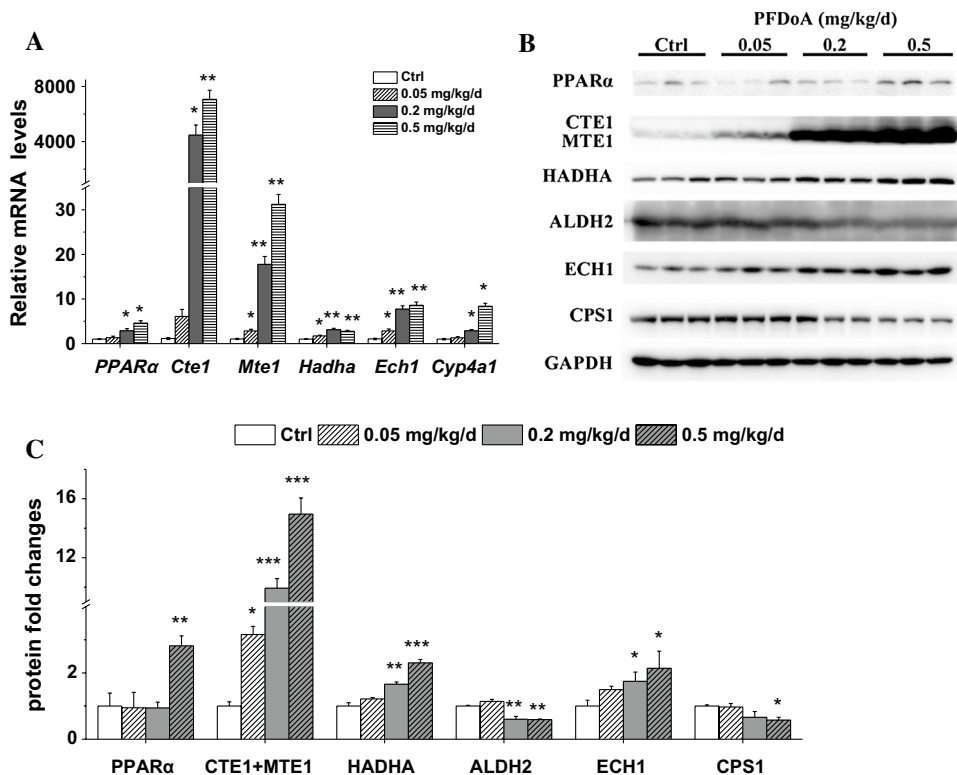
To further explore the role of PPARα in oxidative stress induced by PFDoA, we first measured the transcriptional expression of PPARα and its key target genes. The

mRNA levels of PPARα and target genes such as *Cte1*, *Mte1*, *Hadha*, *Ech1* and *Cyp4a1* all increased significantly in a dose-dependent manner (Fig. 3a). We then measured the protein levels of PPARα and its key target genes (see Fig. 1b) using western blot analysis (Fig. 3b). The protein levels of PPARα's target genes, including CTE1/MTE1, HADHA and ECH1, in rat livers increased in a dose-dependent manner after PFDoA exposure, though a decrease was observed in the protein levels of CPS1 and ALDH2 (Fig. 3c). Interestingly, the protein levels of PPARα increased in the livers of rats dosed with 0.5 mg/kg/day of PFDoA (Fig. 3c).

Content of ROS and activation of PPARα in rat primary hepatocytes exposed to PFDoA

To determine whether the activation of PPARα affected ROS production in rat liver exposed to PFDoA, PPARα antagonist (GW6471) and PPARα agonist (WY14643) were used to treat rat primary hepatocytes. Cells were incubated with 10 µM GW6471 for 24 h, after which the media were removed and the cells were washed three times with PBS and then treated with PFDoA for 24 h. The ROS content significantly increased in both the PFDoA- and GW6471-treated groups compared with that of the control group. When hepatocytes were incubated with GW6471, then treated with 75 µM PFDoA, the ROS content was greater than that in cells treated only with PFDoA (Fig. 4a, b). The mRNA levels of PPARα did not significantly change among the treated groups (PFDoA, GW6471, GW6471 plus PFDoA); however, the mRNA levels of its downstream genes, such as *Cte1*, *Mte1* and *Cyp4a1*, increased in the hepatocytes treated with PFDoA only and decreased in the hepatocytes treated with GW6471 only compared with those of the control group (Fig. 4c). The mRNA levels of these genes increased in the hepatocytes treated with GW6471 plus PFDoA compared with those of GW6471 only group (Fig. 4c). Conversely, the ROS content in the rat primary liver treated with WY14643 only decreased compared with that of both the control group

Fig. 3 **a** Transcriptional levels of PPARα and its target genes (*Cte1*, *Mte1*, *Ech1*, *Hadha* and *Cyp4a1*) in rat liver after PFDoA treatment. *Each bar* represents the mean ± SE of six samples per treatment. **p < 0.05; **p < 0.01* (control group vs PFDoA-treated groups). **b** Protein levels of PPARα, CTE1 + MTE1, HADHA, ALDH2, ECH1 and CPS1 in rat livers after PFDoA treatment. Protein intensities were normalized to the corresponding GAPDH level. **c** Results from densitometry analysis of the western blots in **b**. *Each bar* represents the mean ± SE of six samples per treatment. **p < 0.05; **p < 0.01* (control group vs PFDoA-treated groups)

and PFDoA-treated group (Fig. 4d, e). The mRNA levels of PPARα's downstream genes (*Cte1*, *Mte1* and *Cyp4a1*) were significantly increased in the WY14643-treated groups compared with those of the control and PFDoA-treated group, although the mRNA levels of PPARα were induced only by PFDoA. The mRNA levels of *Cte1*, *Mte1* and *Cyp4a1* in the WY14643 plus PFDoA-treated groups were significantly decreased compared with those of the WY14643-treated only group and increased compared with those of the PFDoA-treated group (Fig. 4f). These results suggest that activation of PPARα may play a protection role in regulating ROS production in rat hepatocytes exposed to PFDoA.

Increased ROS content in PPARα knocked-down rat primary hepatocytes exposed to PFDoA

To further explore the function of PPARα in livers exposed to PFDoA, we conducted lentivirus-mediated RNAi of PPARα in rat primary hepatocytes. We first constructed PPARα-RFP reporter plasmids by fusing rat PPARα cDNA for identification of efficient PPARα (i) sequences (Table S2 in the SI). The qRT-PCR results showed that PPARα (i)-4 was the most effective RNAi vector (Fig. 5a).

The selected RNAi vectors were subcloned into pLenti6.3/V5-DEST vectors by GateWay recombination (Fig. 5b). The lentiviruses containing Lenti-miPPARα RNAi vectors were packaged by co-transfection with

ViraPower™ lentiviral expression systems into 293FT cells (Fig. 5c). MOI was assayed by infection of rat primary hepatocytes with a serial dilution of lentivirus stock. The result showed that MOI 30 was suitable for the successful transduction of rat primary hepatocytes (Fig. 5d).

Rat primary hepatocytes were successfully infected with mock (negative control, Lenti-NC) and Lenti-miPPARα lentiviruses, showing bright green fluorescence without morphological abnormalities under a fluorescent microscope (Fig. 6a). The qRT-PCR results showed that the RNAi efficiency was 82 and 83 % with vehicle and PFDoA, respectively (Fig. 6b). Next, we examined the mRNA expression levels of PPARα target genes in rat primary hepatocytes exposed to PFDoA in vitro. Ninety-six hours after lentivirus infection, the transcriptional levels of *Cte1*, *Mte1*, *Hadha*, *Ech1* and *Cps1* were significantly down-regulated in PPARα knocked-down rat hepatocytes compared with those of the control group. Treatment of rat primary hepatocytes 96 h post-lentivirus infection with PFDoA for 24 h yielded similar trends (Fig. 6c), while the mRNA expression levels of *Aldh2* did not show significant change.

The protein level of PPARα was markedly reduced in the rat primary hepatocytes infected with Lenti-miPPARα lentivirus for 8 days compared with the mock group, as were the protein levels of CTE1 and MTE1. After infection with Lenti-miPPARα lentivirus for 8 days, followed by treatment with PFDoA for 24 h, the protein levels of CTE1
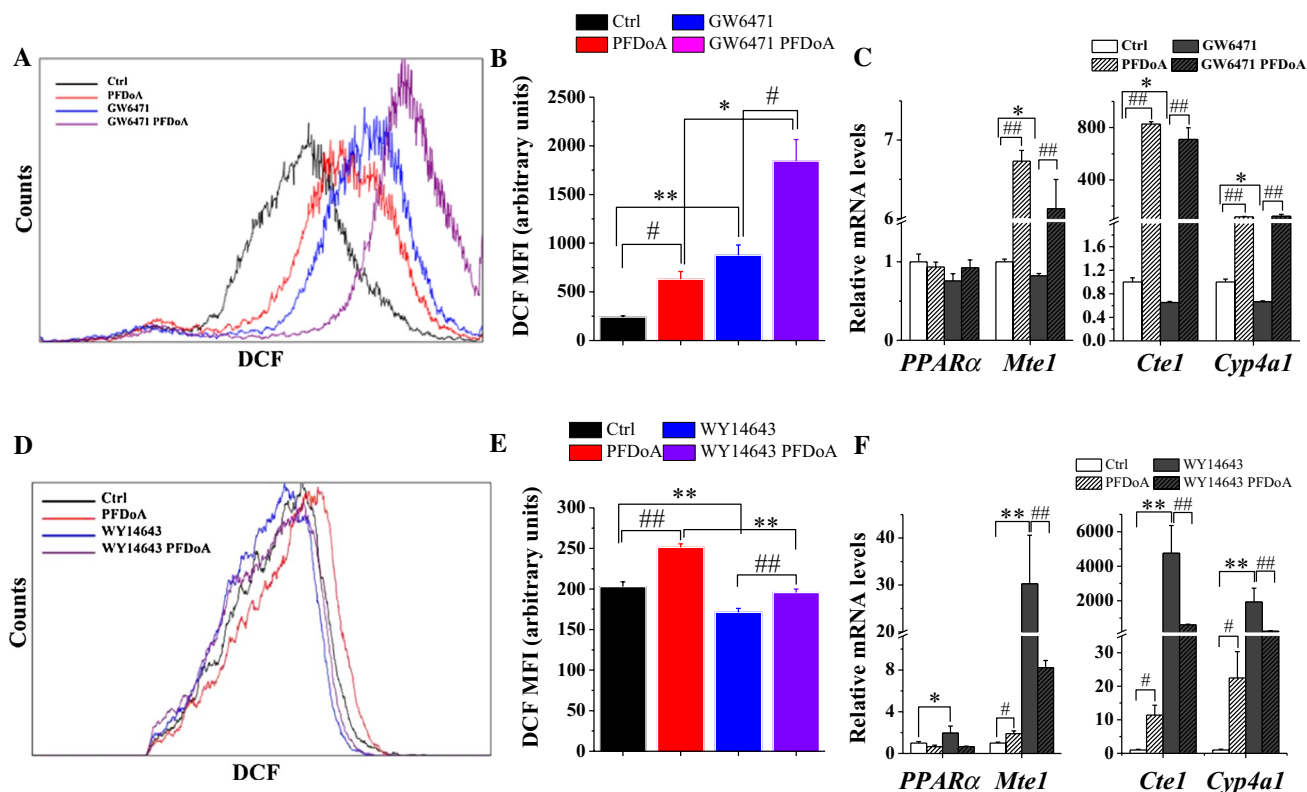
Fig. 4 Reactive oxygen species (ROS) content assay of rat hepatocytes exposed to PFDoA. **a** ROS content of rat hepatocytes pretreated with PPARα antagonist GW6471 measured by flow cytometry using molecular probe H$_2$DCFA. **b** Mean fluorescence intensity of DCF measured by flow cytometry. **c** Quantitative RT-PCR analysis of mRNA expression levels in rat primary hepatocytes pre-treated with GW6471 and exposed to PFDoA. **d** ROS content of rat hepatocytes pre-treated with PPARα agonist WY14643 measured by flow cytometry using molecular probe H$_2$DCFA. **e** Mean fluorescence intensity of DCF measured by flow cytometry. **f** qRT-PCR analysis of mRNA expression levels in rat primary hepatocytes treated with WY14643 and PFDoA. Mean ± SEM; $n = 3$ (*$p < 0.05$; **$p < 0.01$)

and MTE1 in rat hepatocytes increased compared with those of the Lenti-miPPARα vehicle group but decreased compared with those of the PFDoA-treated mock group (Fig. 7a, b). However, after infection with Lenti-miPPARα lentivirus for 8 days, the protein levels of HADHA, ECH1 and CPS1 were significantly increased compared with those of the mock group, while ALDH2 exhibited no significant change. After PPARα knockdown for 8 days, followed by treatment with PFDoA for 24 h, the protein levels of ECH1 and CPS1 decreased compared with those of the PFDoA-untreated Lenti-miPPARα group. However, ALDH2 significantly increased in rat hepatocytes. These results implied that CTE1 and MTE1 were positively regulated by PPARα, and HADHA, CPS1 and ECH1 were negatively regulated by PPARα. These findings are consistent with the pathway analysis of the regulatory network of the PPARα downstream proteins (Figs. 1b, 3), except for ECH1 and HADHA, which may be regulated by other factors. The detailed mechanism needs further exploration.

We further investigated the content of ROS in PPARα knocked-down rat primary hepatocytes. Due to the green color of GFP transduced by lentivirus, DHE was used for ROS measurement. The content of ROS was markedly increased in the rat primary hepatocytes infected with Lenti-miPPARα lentivirus for 8 days compared with the mock (Lenti-NC) group. After infection with Lenti-miPPARα lentivirus for 8 days followed by treatment with PFDoA for 24 h, the content of ROS in rat hepatocytes did not increase compared with that of the Lenti-miPPARα vehicle group but still increased when compared with that of the PFDoA-treated mock group (Fig. 8a–c). These results were similar to those of the GW6471-treated groups.

We next measured the transcriptional levels of genes involved in ROS scavenging in rat primary hepatocytes. Results showed that the transcriptional levels of *Sod2* and *Gpx4* were markedly increased, while the levels of *Cat* decreased in the rat primary hepatocytes infected with Lenti-miPPARα lentivirus for 8 days compared with the mock (Lenti-NC) group. After infection with Lenti-miPPARα lentivirus for 8 days, followed by treatment with PFDoA for 24 h, the transcriptional levels of these genes in rat hepatocytes did not increase compared with those
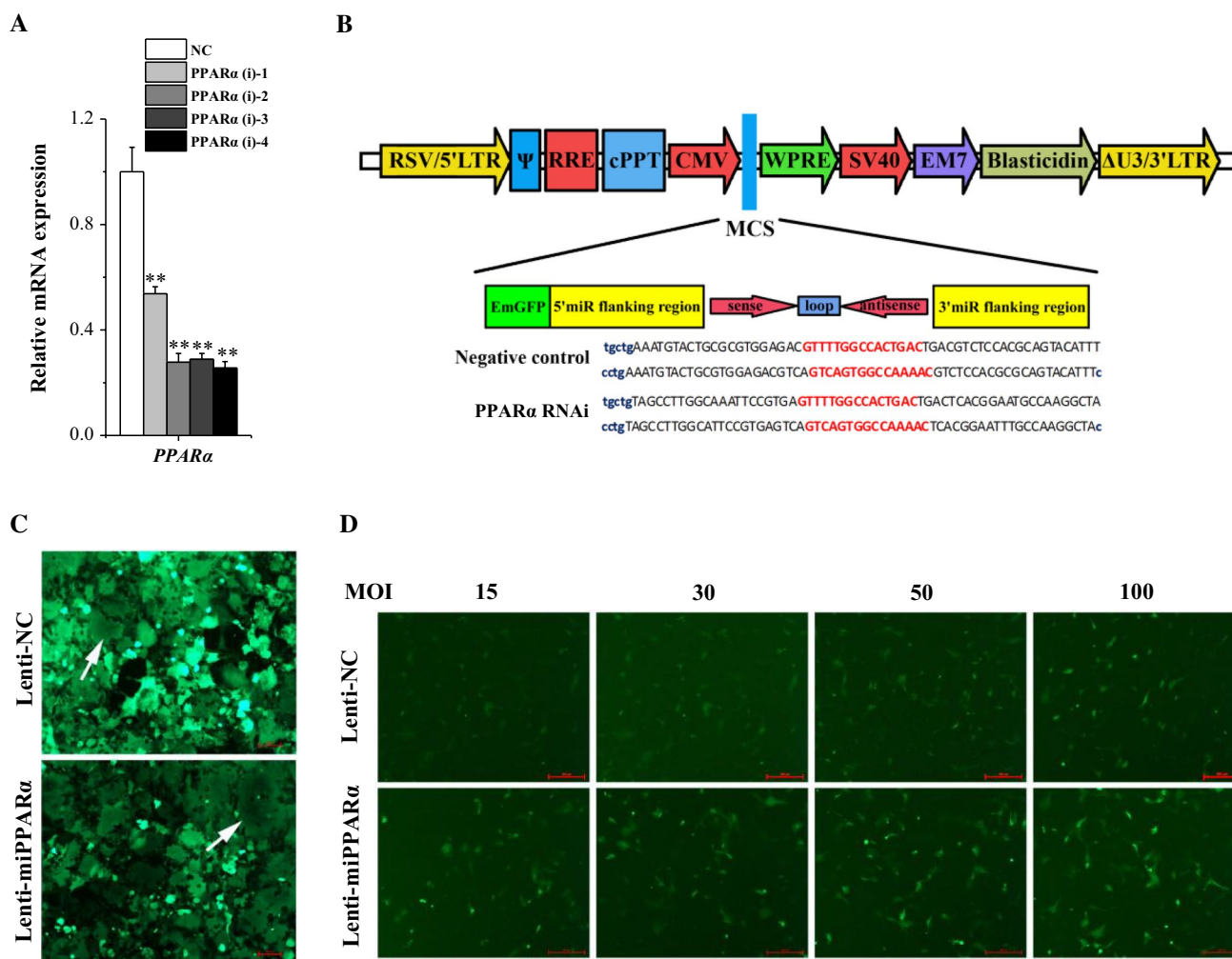
Fig. 5 Lentivirus design based on peroxisome proliferator-activated receptor alpha (PPARα) RNAi vectors. **a** Knockdown efficiency was verified by qRT-PCR assays, PPARα (i)-4 was the most effective sequence among each four candidates ($p < 0.05$) (candidate design is listed in Supplemented Information S1). *NC* indicates cells transfected with negative control RNAi vector, PPARα *(i)-1, -2, -3,* and *-4* indicates cells transfected with PPARα (i)-1, -2, -3, and -4 vectors, respectively. **b** Schematic representation of microRNA (miRNA) lentiviral vector and oligonucleotide sequences of screened candidates for constructing miPPARα lentiviruses targeting PPARα. *Blue characters* indicate sequences of the vector, *red characters* are loop sequences of the miRNA, and *flanked black characters* are the palindromic core sequences. Framework of the lentiviral RNAi vectors was pLenti6.3/V5-DEST vectors (Invitrogen Life Technology). **c** Successful packaging of lentivirus. *Arrows* show the multinucleated cells known as "syncytia". **d** A range of MOIs (15, 30, 50 and 100) were used to determine the MOI required to achieve the optimal infection effect in rat primary hepatocytes. MOI 30 was chosen for the experiment. *Scale bar* 500 µm (color figure online)

of the Lenti-miPPARα vehicle group but change trends of these genes were similar to those of the PFDoA-treated mock group (Fig. 8d). These results were consistent with the ROS increase in rat primary hepatocytes when PPARα was knocked down.

Discussion

In the present study, 70 identified proteins were significantly altered in the 0.5 mg/kg/day PFDoA group. Among which, 28 were significantly altered in both the 0.2 and

0.5 mg/kg/day PFDoA groups with a similar changing trend, and the fold changes in the higher-dose group were higher than those in the lower-dose group. This suggests that the effect of PFDoA on the liver was dose dependent. Western blot analysis validated the reliability of the DIGE results and showed that the altered proteins could provide comprehensive information on the translational levels of hepatotoxicity in male rats after subchronic exposure of PFDoA.

PFOA is known to activate PPARα and is considered a critical step in the mode of action by which PFOA induces hepatotoxicity in rodents, including liver enlargement,
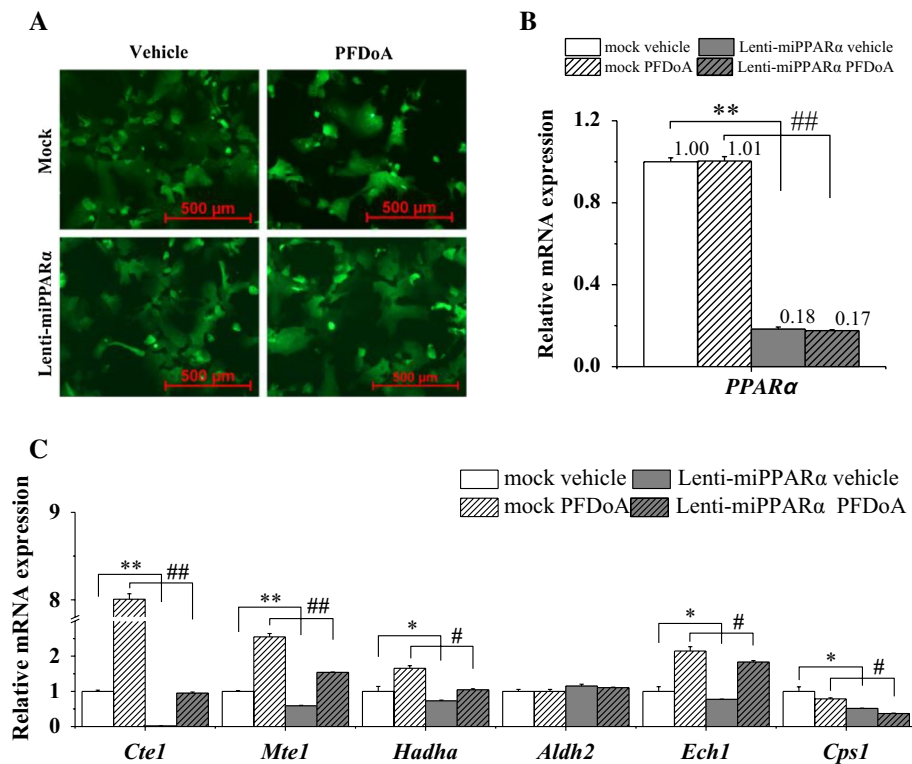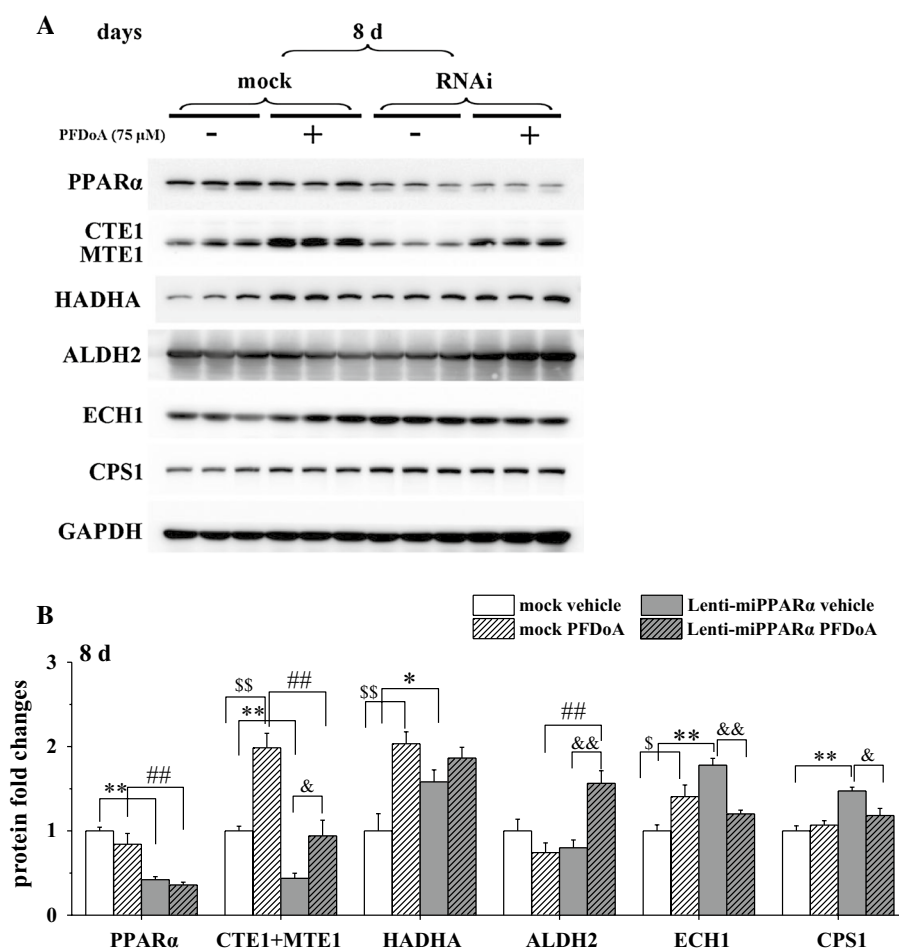
Fig. 6 Rat primary hepatocytes infected with miPPARα lentiviruses. **a** Rat primary hepatocytes were infected with lentiviruses at MOI 30; mock is the lentivirus of the negative control, Lenti-miPPARα indicates the lentivirus of miPPARα lentiviral vectors. Vehicle was 75 μM ethanol in media, PFDoA was 75 μM in media. Green fluorescence was the GFP from the lentiviruses, which guaranteed successful delivery of RNAi vectors by the lentiviruses. *Scale bar* 500 μm. **b** PPARα mRNA expression in rat primary hepatocytes was successfully knocked-down post-lentivirus infection of 96 h. *Mock vehicle* indicates cells infected with negative control lentivirus without exposure of PFDoA, only vehicle, *mock PFDoA* indicates cells infected with negative control and exposed to PFDoA, *mi*PPARα *vehicle* indicates cells infected with Lenti-miPPARα lentivirus without exposure of PFDoA for 24 h, only vehicle, *mi*PPARα *PFDoA* indicates cells infected with Lenti-miPPARα lentivirus and treatment with PFDoA for 24 h. Relative mRNA expression of PPARα was knocked down by 82 % compared with that of the mock vehicle group after Lenti-miPPARα infection; and knocked down by 83 % compared with that of the mock PFDoA group after Lenti-miPPARα infection and PFDoA exposure. **c** Relative mRNA expression variations of PPARα downstream genes after PPARα was knocked down by Lenti-miPPARα infection. Mean ± SEM; $n = 3$ (*$p < 0.05$; **$p < 0.01$; mock vehicle group vs Lenti-miPPARα vehicle groups), (#$p < 0.05$; ##$p < 0.01$; mock PFDoA group vs Lenti-miPPARα PFDoA groups)

liver cancer and tumors and fatty acid metabolism disorders (Elcombe et al. 2012; Lau et al. 2007). In our previous studies, PFDoA was also found to activate the mRNA levels of PPARs and its target genes associated with fatty acid homeostasis, which might contribute to the hepatic steatosis observed (Ding et al. 2009; Zhang et al. 2008). In this study, four up-regulated proteins (CTE1, MTE1, HADHA and ECH1) were related to lipid metabolism, with all previously reported to be target genes of PPARα (Desvergne and Wahli 1999; Mandard et al. 2004). Additionally, two down-regulated proteins (CPS1 and ALDH2) involved in amino acid and glucose metabolism, respectively, were found to be related to PPARα by Pathway Studio analysis. Interestingly, both the mRNA and protein levels of CTE1 and MTE1 were increased greatly following PFDoA exposure compared with those of other genes. Thus, we successfully transferred the miPPARα plasmid into rat primary

hepatocytes by lentivirus infection to knock down both the mRNA and protein expression of PPARα and determine whether PFDoA induced CTE1 and MTE1, or other proteins, based on PPARα activation. Hunt et al. (2000) reported that CTE1 and MTE1 were induced at the mRNA level in fasting PPARα-null mice, but the increase in CTE1 was mainly independent of PPARα in the liver. A recent study evaluated the gene profile alterations of hepatocytes in PPAR knockout or wild-type mice given oral daily doses of PFOA and WY-14643 for 7 days (Rosen et al. 2008a, b, 2010). The induction of CTE1, MTE1 and HADHA observed only in the wild-type mice showed a completely PPARα-dependent pathway. However, ECH1 and CPS1 were regulated not only in wild-type mice treated by PFOA but also knockout mice to a lesser extent, suggesting that these two genes might be partially regulated by PPARα. This was consistent with our study, which showed that the

Fig. 7 Western blot analysis of CTE1 + MTE1, HADHA, ALDH2, ECH1 and CPS1 protein levels in PPARα knocked-down rat primary hepatocytes after 75 μM PFDoA exposure for 24 h. **a** Effect of PPARα knockdown on its downstream proteins in rat primary hepatocytes. Cells were harvested 8 day post-lentivirus infection, respectively. **b** Protein intensities normalized to the corresponding GAPDH level. Densitometry analysis was performed using Quantity One software. *Each bar* represents the mean ± SE of three samples per treatment. Mean ± SEM; n = 3 (*p < 0.05; **p < 0.01; mock vehicle group vs Lenti-miPPARα vehicle groups), (#p < 0.05; ##p < 0.01; mock PFDoA group vs Lenti-miPPARα PFDoA groups), ($p < 0.05; $$p < 0.01; mock vehicle group vs mock PFDoA groups; &p < 0.05; &&p < 0.01; Lenti-miPPARα vehicle groups vs Lenti-miPPARα PFDoA groups)
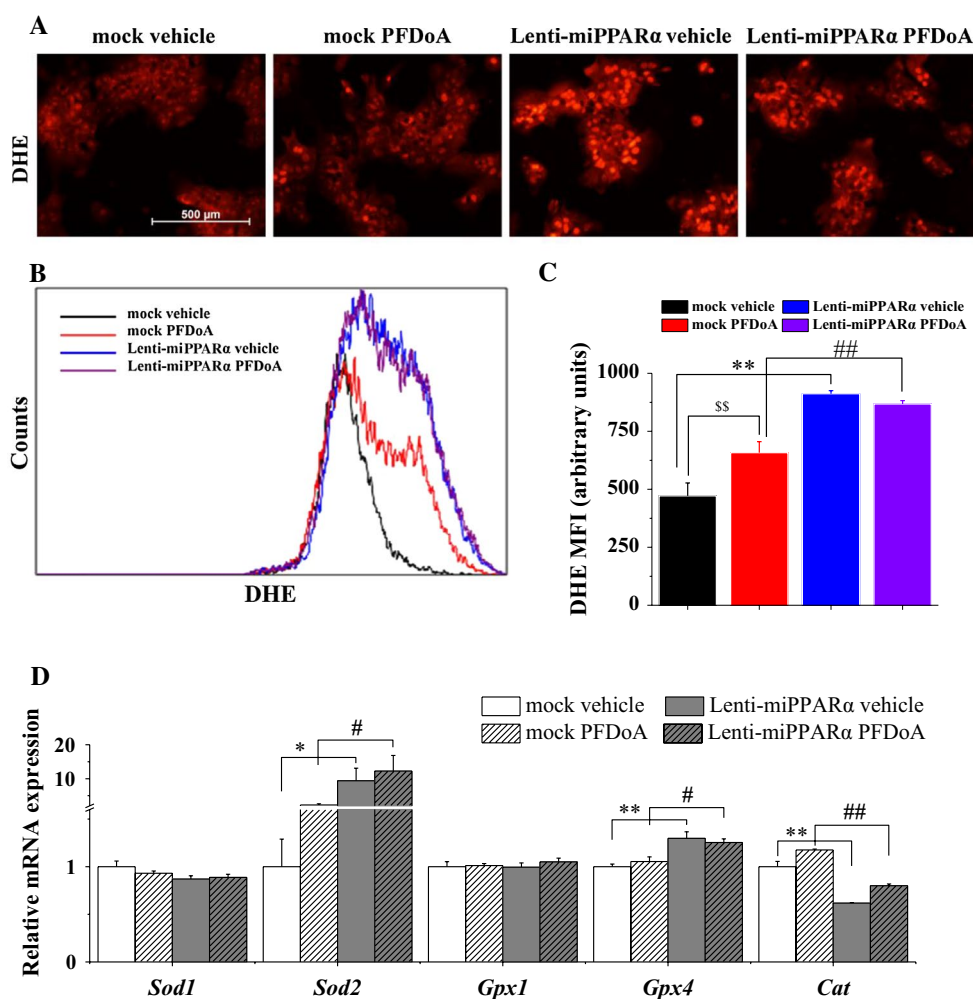

regulations of CTE1, MTE1, HADHA, ECH1 and CPS1 mRNA levels in rat liver exposed to PFDoA were related to PPARα. In addition, other transcription factors such as activated/androstane receptor (CAR) and pregnane X receptor (PXR) might be involved in the effect of PFDoA (Bjork et al. 2011; Ren et al. 2009). For protein levels, only CTE1 and MTE1 levels decreased obviously in PPARα knocked-down hepatocytes after PFDoA exposure compared with those in wild-type primary hepatocytes, although no obvious activation of PPARα by PFDoA was observed. These results suggest that CTE1 and MTE1 were more sensitive to PFASs and had a potential to use as a biological indicator of PFASs.

Furthermore, 16 of the differentially expressed proteins after PFDoA treatment were related to stress response, including HSPs, PRXs and PDIA6. Heat-shock proteins, originally identified as heat-inducible gene products, are a family of highly conserved proteins that respond to a wide variety of stresses, including oxidative stress. Under oxidative stress, hepatic cells can produce high levels of stress response proteins, including HSPs, which protect against free radical insult (Liu et al. 2015; Ogi et al. 1999). In this study, protein levels of HSPs (except spot

281) were all induced in the high PFDoA dose group, indicating that a certain degree of oxidative stress might occur in rat liver exposed to PFDoA. Multiple studies have demonstrated that PFAS exposure can induce excessive ROS in various cells (Eriksen et al. 2010; Liu et al. 2007; Reistad et al. 2013; Yang et al. 2014). In our study, ROS content increased in rat primary hepatocytes exposed to PFDoA. Additionally, significantly increased SOD activity and TBARS production in the 0.5 mg/kg/day PFDoA group reflected ROS production by PFDoA in vivo. It has been reported that peroxisome proliferation could be of sufficient magnitude to lead to oxidative damage in macromolecules, with PPARα activation as a causal first step (Yeldandi et al. 2000). In livers with peroxisome proliferation, fatty acyl-CoA oxidase (ACOX) and CYP4A1, two well-known PPARα target genes and important enzymes of fatty acid oxidation, have been considered the major sources of H_2O_2 contributing to sustained intracellular oxidative damage in the livers of rats and mice (Nemali et al. 1989). Our previous study also showed that the mRNA levels of ACOX and CYP4A1 were significantly induced after subchronic and subacute PFDoA exposure (Ding et al. 2009; Zhang et al. 2008). In addition, the activities of CAT

Fig. 8 Suppression of PPARα increased ROS in rat primary hepatocytes exposed to PFDoA. **a** Fluorescent images of lentivirus infected rat hepatocytes stained with DHE. *Scale bar* 500 μm. **b** ROS content of rat hepatocytes infected with lentiviruses measured by flow cytometry using molecular probe DHE. **c** Mean fluorescence intensity of DHE measured by flow cytometry. **d** Quantitative RT-PCR analysis of mRNA expression levels in rat primary hepatocytes infected with lentiviruses and exposed to PFDoA. Mean ± SEM; $n = 3$ (*$p < 0.05$; **$p < 0.01$; mock vehicle group vs Lenti-miPPARα vehicle groups), (#$p < 0.05$; ##$p < 0.01$; mock PFDoA group vs Lenti-miPPARα PFDoA groups), ($p < 0.05$; $$p < 0.01$; mock vehicle group vs mock PFDoA groups)

and GPx, two H_2O_2-degrading enzymes, were markedly reduced in rat livers in the 0.5 mg/kg/day PFDoA group, which further led to excess oxidative stress. Taken together, we speculated that activation of PPARα might be the initial cause of oxidative stress induced by PFDoA in the rat liver.

The in vitro experiments further verified the relationship of PPARα with oxidative stress in rat primary hepatocytes induced by PFDoA. Interestingly, the PPARα antagonist GW6471, as well as Lenti-miPPARα transfection, attenuated the induction of mRNA levels in PPARα target genes (CTE1, MTE1 and CYP4A1) in both the control and PFDoA-exposed hepatocytes, which was associated with increased ROS accumulation. Furthermore, ROS content in rat hepatocytes was significantly decreased when pretreated with PPARα agonist WY14643 in both the control and PFDoA-treated groups, and the corresponding PPARα targeted genes were all up-regulated. The induction of GPx and SOD2 levels might be a response to ROS accumulation in primary hepatocytes. These results implied that PPARα could inhibit ROS accumulation in rat hepatocytes exposed to PFDoA. An increasing body of evidence suggests that

activation of PPARα could protect the liver against chemical-induced stress or damage (Anderson et al. 2002; Chen et al. 2000; Mehendale 2000), consistent with our in vitro studies. Minata et al. (2010) reported that PFOA elevated the levels of 8-hydroxydeoxyguanosine, an indicator of oxidative DNA damage, in the liver of PPARα-null mice, but did not increase 8-hydroxydeoxyguanosine levels in the livers of wild-type mice. However, the levels of ALT and AST in PPARα-null mice were lower than that in wild-type mice after exposure to 12.5 and 25 μmol/kg PFOA, but were increased more than twofold that of wild-type mice exposed to 50 μmol/kg PFOA (Minata et al. 2010). Thus, PPARα played an important role not only in induction of oxidative stress but also in protection against the liver injury. A balance might exist between the double functions of PPARα; however, other pathways involved in ROS generation and the detailed mechanism of PPARα protection against oxidative damage induced by PFDoA remains unclear and needs further study.

In summary, 73 differentially expressed proteins were identified in the rat liver after PFDoA exposure and were

related to lipid metabolism, stress response and inflammation. In addition, PFDoA exposure led to oxidative stress in the rat liver, including ROS accumulation, induction of SOD activity, inhibition of GPx activity and increased lipid peroxidation. PPARα might play an important role in the protection against ROS accumulation in the rat liver induced by PFDoA.

References

Abbott BD, Wolf CJ, Das KP et al (2009) Developmental toxicity of perfluorooctane sulfonate (PFOS) is not dependent on expression of peroxisome proliferator activated receptor-alpha (PPAR alpha) in the mouse. Reprod Toxicol (Elmsford, NY) 27(3–4):258–265. doi:10.1016/j.reprotox.2008.05.061

Alban A, David SO, Bjorkesten L et al (2003) A novel experimental design for comparative two-dimensional gel analysis: two-dimensional difference gel electrophoresis incorporating a pooled internal standard. Proteomics 3(1):36–44

Anderson SP, Yoon L, Richard EB, Dunn CS, Cattley RC, Corton JC (2002) Delayed liver regeneration in peroxisome proliferator-activated receptor-alpha-null mice. Hepatology 36(3):544–554. doi:10.1053/jhep.2002.35276

Bjork JA, Butenhoff JL, Wallace KB (2011) Multiplicity of nuclear receptor activation by PFOA and PFOS in primary human and rodent hepatocytes. Toxicology 288(1–3):8–17. doi:10.1016/j.tox.2011.06.012

Calafat AM, Wong LY, Kuklenyik Z, Reidy JA, Needham LL (2007) Polyfluoroalkyl chemicals in the US population: data from the National Health and Nutrition Examination Survey (NHANES) 2003–2004 and comparisons with NHANES 1999–2000. Environ Health Perspect 115(11):1596–1602. doi:10.1289/ehp.10598

Chen C, Hennig GE, Whiteley HE, Corton JC, Manautou JE (2000) Peroxisome proliferator-activated receptor alpha-null mice lack resistance to acetaminophen hepatotoxicity following clofibrate exposure. Toxicol Sci 57(2):338–344

Desvergne B, Wahli W (1999) Peroxisome proliferator-activated receptors: nuclear control of metabolism. Endocr Rev 20(5):649–688

DeWitt JC, Shnyra A, Badr MZ et al (2009) Immunotoxicity of perfluorooctanoic acid and perfluorooctane sulfonate and the role of peroxisome proliferator-activated receptor alpha. Crit Rev Toxicol 39(1):76–94

Ding L, Hao F, Shi Z et al (2009) Systems biological responses to chronic perfluorododecanoic acid exposure by integrated metabonomic and transcriptomic studies. J Proteome Res 8(6):2882–2891. doi:10.1021/pr9000256

Dinglasan JA, Bailey M, Park JB, Dhirani AA (2004) Differential conductance switching of planar tunnel junctions mediated by oxidation/reduction of functionally protected ferrocene. J Am Chem Soc 126(20):6491–6497. doi:10.1021/ja0394176

Elcombe CR, Elcombe BM, Foster JR, Chang SC, Ehresman DJ, Butenhoff JL (2012) Hepatocellular hypertrophy and cell proliferation in Sprague–Dawley rats from dietary exposure to potassium perfluorooctanesulfonate results from increased expression of xenosensor nuclear receptors PPARalpha and CAR/PXR. Toxicology 293(1–3):16–29. doi:10.1016/j.tox.2011.12.014

Eriksen KT, Raaschou-Nielsen O, Sorensen M, Roursgaard M, Loft S, Moller P (2010) Genotoxic potential of the perfluorinated chemicals PFOA, PFOS, PFBS, PFNA and PFHxA in human HepG2 cells. Mutat Res 700(1–2):39–43. doi:10.1016/j.mrgentox.2010.04.024

Evans RM, Barish GD, Wang YX (2004) PPARs and the complex journey to obesity. Nat Med 10(4):355–361. doi:10.1038/nm1025

Fujii Y, Yan J, Harada KH et al (2012) Levels and profiles of long-chain perfluorinated carboxylic acids in human breast milk and infant formulas in East Asia. Chemosphere 86(3):315–321. doi:10.1016/j.chemosphere.2011.10.035

Giesy JP, Kannan K (2001) Global distribution of perfluorooctane sulfonate in wildlife. Environ Sci Technol 35(7):1339–1342

Gorrochategui E, Perez-Albaladejo E, Casas J, Lacorte S, Porte C (2014) Perfluorinated chemicals: differential toxicity, inhibition of aromatase activity and alteration of cellular lipids in human placental cells. Toxicol Appl Pharmacol 277(2):124–130. doi:10.1016/j.taap.2014.03.012

Hansen KJ, Clemen LA, Ellefson ME, Johnson HO (2001) Compound-specific, quantitative characterization of organic fluorochemicals in biological matrices. Environ Sci Technol 35(4):766–770

Houde M, Martin JW, Letcher RJ, Solomon KR, Muir DC (2006) Biological monitoring of polyfluoroalkyl substances: a review. Environ Sci Technol 40(11):3463–3473

Houde M, De Silva AO, Muir DC, Letcher RJ (2011) Monitoring of perfluorinated compounds in aquatic biota: an updated review. Environ Sci Technol 45(19):7962–7973. doi:10.1021/es104326w

Hundley SG, Sarrif AM, Kennedy GL (2006) Absorption, distribution, and excretion of ammonium perfluorooctanoate (APFO) after oral administration to various species. Drug Chem Toxicol 29(2):137–145

Hunt MC, Lindquist PJ, Peters JM, Gonzalez FJ, Diczfalusy U, Alexson SE (2000) Involvement of the peroxisome proliferator-activated receptor alpha in regulating long-chain acyl-CoA thioesterases. J Lipid Res 41(5):814–823

Ishii T, Warabi E, Yanagawa T (2012) Novel roles of peroxiredoxins in inflammation, cancer and innate immunity. J Clin Biochem Nutr 50(2):91–105. doi:10.3164/jcbn.11-109

Kersten S, Desvergne B, Wahli W (2000) Roles of PPARs in health and disease. Nature 405(6785):421–424. doi:10.1038/35013000

Kleszczynski K, Gardzielewski P, Mulkiewicz E, Stepnowski P, Skladanowski AC (2007) Analysis of structure–cytotoxicity in vitro relationship (SAR) for perfluorinated carboxylic acids. Toxicol In Vitro 21(6):1206–1211. doi:10.1016/j.tiv.2007.04.020

Kudo N, Suzuki E, Katakura M, Ohmori K, Noshiro R, Kawashima Y (2001) Comparison of the elimination between perfluorinated fatty acids with different carbon chain length in rats. Chem Biol Interact 134(2):203–216

Kudo N, Suzuki-Nakajima E, Mitsumoto A, Kawashima Y (2006) Responses of the liver to perfluorinated fatty acids with different carbon chain length in male and female mice: in relation to induction of hepatomegaly, peroxisomal beta-oxidation and microsomal 1-acylglycerophosphocholine acyltransferase. Biol Pharm Bull 29(9):1952–1957

Lam NH, Cho CR, Lee JS et al (2014) Perfluorinated alkyl substances in water, sediment, plankton and fish from Korean rivers and lakes: a nationwide survey. Sci Total Environ 491–492:154–162. doi:10.1016   /j.scitotenv.2014.01.045

Lau C, Anitole K, Hodes C, Lai D, Pfahles-Hutchens A, Seed J (2007) Perfluoroalkyl acids: a review of monitoring and toxicological findings. Toxicol Sci 99(2):366–394. doi:10.1093/toxsci/kfm128

Lin AY, Panchangam SC, Tsai YT, Yu TH (2014) Occurrence of perfluorinated compounds in the aquatic environment as found in science park effluent, river water, rainwater, sediments, and bottissues. Environ Monit Assess 186(5):3265–3275. doi:10.1007/s10661-014-3617-9

Liu C, Yu K, Shi X et al (2007) Induction of oxidative stress and apoptosis by PFOS and PFOA in primary cultured hepatocytes of freshwater tilapia (*Oreochromis niloticus*). Aquat Toxicol (Amsterdam, Neth) 82(2):135–143. doi:10.1016/j.aquatox.2007.02.006

Liu W, Chen S, Quan X, Jin YH (2008) Toxic effect of serial perfluorosulfonic and perfluorocarboxylic acids on the membrane system of a freshwater alga measured by flow cytometry. Environ Toxicol Chem 27(7):1597–1604. doi:10.1897/07-459

Liu CP, Fu J, Xu FP, Wang XS, Li S (2015) The role of heat shock proteins in oxidative stress damage induced by Se deficiency in chicken livers. Biometals 28(1):163–173. doi:10.1007/s10534-014-9812-x

Mandard S, Muller M, Kersten S (2004) Peroxisome proliferator-activated receptor alpha target genes. Cell Mol Life Sci 61(4):393–416. doi:10.1007/s00018-003-3216-3

Martin JW, Mabury SA, Solomon KR, Muir DC (2003) Bioconcentration and tissue distribution of perfluorinated acids in rainbow trout (*Oncorhynchus mykiss*). Environ Toxicol Chem 22(1):196–204

Martin JW, Smithwick MM, Braune BM, Hoekstra PF, Muir DC, Mabury SA (2004) Identification of long-chain perfluorinated acids in biota from the Canadian Arctic. Environ Sci Technol 38(2):373–380

Mehendale HM (2000) PPAR-alpha: a key to the mechanism of hepatoprotection by clofibrate. Toxicol Sci 57(2):187–190

Minata M, Harada KH, Karrman A et al (2010) Role of peroxisome proliferator-activated receptor-alpha in hepatobiliary injury induced by ammonium perfluorooctanoate in mouse liver. Ind Health 48(1):96–107

Naile JE, Khim JS, Wang T et al (2010) Perfluorinated compounds in water, sediment, soil and biota from estuarine and coastal areas of Korea. Environ Pollut 158(5):1237–1244. doi:10.1016/j.envpol.2010.01.023

Nemali MR, Reddy MK, Usuda N et al (1989) Differential induction and regulation of peroxisomal enzymes: predictive value of peroxisome proliferation in identifying certain nonmutagenic carcinogens. Toxicol Appl Pharmacol 97(1):72–87

Nikitin A, Egorov S, Daraselia N, Mazo I (2003) Pathway studio—the analysis and navigation of molecular networks. Bioinformatics 19(16):2155–2157. doi:10.1093/bioinformatics/btg290

Ogi S, Tanji N, Iseda T, Yokoyama M (1999) Expression of heat shock proteins in developing and degenerating rat testes. Arch Androl 43(3):163–171

Ohmori K, Kudo N, Katayama K, Kawashima Y (2003) Comparison of the toxicokinetics between perfluorocarboxylic acids with different carbon chain length. Toxicology 184(2–3):135–140

Reistad T, Fonnum F, Mariussen E (2013) Perfluoroalkylated compounds induce cell death and formation of reactive oxygen species in cultured cerebellar granule cells. Toxicol Lett 218(1):56–60. doi:10.1016/j.toxlet.2013.01.006

Ren H, Vallanat B, Nelson DM et al (2009) Evidence for the involvement of xenobiotic-responsive nuclear receptors in transcriptional effects upon perfluoroalkyl acid exposure in diverse species. Reprod Toxicol 27(3–4):266–277. doi:10.1016/j.reprotox.2008.12.011

Rich CD, Blaine AC, Hundal L, Higgins CP (2015) Bioaccumulation of perfluoroalkyl acids by earthworms (*Eisenia fetida*) exposed to contaminated soils. Environ Sci Technol. doi:10.1021/es504152d

Rosen ED, Sarraf P, Troy AE et al (1999) PPAR gamma is required for the differentiation of adipose tissue in vivo and in vitro. Mol Cell 4(4):611–617

Rosen MB, Abbott BD, Wolf DC et al (2008a) Gene profiling in the livers of wild-type and PPARalpha-null mice exposed to perfluorooctanoic acid. Toxicol Pathol 36(4):592–607. doi:10.1177/0192623308318208

Rosen MB, Lee JS, Ren H et al (2008b) Toxicogenomic dissection of the perfluorooctanoic acid transcript profile in mouse liver: evidence for the involvement of nuclear receptors PPAR alpha and CAR. Toxicol Sci 103(1):46–56. doi:10.1093/toxsci/kfn025

Rosen MB, Schmid JR, Corton JC et al (2010) Gene expression profiling in wild-type and PPARalpha-null mice exposed to perfluorooctane sulfonate reveals PPARalpha-independent effects. PPAR Res 2010. doi:10.1155/2010/794739

Seacat AM, Thomford PJ, Hansen KJ et al (2003) Sub-chronic dietary toxicity of potassium perfluorooctanesulfonate in rats. Toxicology 183(1–3):117–131

Seglen PO (1976) Preparation of isolated rat liver cells. Methods Cell Biol 13:29–83

Senthilkumar K, Ohi E, Sajwan K, Takasuga T, Kannan K (2007) Perfluorinated compounds in river water, river sediment, market fish, and wildlife samples from Japan. Bull Environ Contam Toxicol 79(4):427–431. doi:10.1007/s00128-007-9243-2

Shen L, Hillebrand A, Wang DQ, Liu M (2012) Isolation and primary culture of rat hepatic cells. J Vis Exp (JoVE) (64). doi:10.3791/3917

Shipley JM, Hurst CH, Tanaka SS et al (2004) trans-activation of PPARalpha and induction of PPARalpha target genes by perfluorooctane-based chemicals. Toxicol Sci 80(1):151–160. doi:10.1093/toxsci/kfh130

Takacs ML, Abbott BD (2007) Activation of mouse and human peroxisome proliferator-activated receptors (alpha, beta/delta, gamma) by perfluorooctanoic acid and perfluorooctane sulfonate. Toxicol Sci 95(1):108–117. doi:10.1093/toxsci/kfl135

Taniyasu S, Kannan K, So MK et al (2005) Analysis of fluorotelomer alcohols, fluorotelomer acids, and short- and long-chain perfluorinated acids in water and biota. J Chromatogr A 1093(1–2):89–97. doi:10.1016/j.chroma.2005.07.053

Thingholm TE, Larsen MR, Ingrell CR, Kassem M, Jensen ON (2008) TiO_2-based phosphoproteomic analysis of the plasma membrane and the effects of phosphatase inhibitor treatment. J Proteome Res 7(8):3304–3313. doi:10.1021/pr800099y

Wetmore BA, Merrick BA (2004) Toxicoproteomics: proteomics applied to toxicology and pathology. Toxicol Pathol 32(6):619–642

Yamada S, Ding Y, Sasaguri Y (2012) Peroxiredoxin 4: critical roles in inflammatory diseases. J UOEH 34(1):27–39

Yang B, Zou W, Hu Z et al (2014) Involvement of oxidative stress and inflammation in liver injury caused by perfluorooctanoic acid exposure in mice. Biomed Res Int 2014:409837. doi:10.1155/2014/409837

Yeldandi AV, Rao MS, Reddy JK (2000) Hydrogen peroxide generation in peroxisome proliferator-induced oncogenesis. Mutat Res 448(2):159–177

Zhang H, Shi Z, Liu Y, Wei Y, Dai J (2008) Lipid homeostasis and oxidative stress in the liver of male rats exposed to perfluorododecanoic acid. Toxicol Appl Pharmacol 227(1):16–25. doi:10.1016/j.taap.2007.09.026

Zhang H, Ding L, Fang X et al (2011) Biological responses to perfluorododecanoic acid exposure in rat kidneys as determined by integrated proteomic and metabonomic studies. PLoS One 6(6):e20862. doi:10.1371/journal.pone.0020862

Zhang W, Liu Y, Zhang H, Dai J (2012) Proteomic analysis of male zebrafish livers chronically exposed to perfluorononanoic acid. Environ Int 42:20–30. doi:10.1016/j.envint.2011.03.002